

Real World Robustness from Systematic Noise

Yan Wang
SenseTime Research
Beijing, Beijing, China
wangyan3@sensetime.com

Yuhang Li
Yale University
New Haven, CT, USA
yuhang.li@yale.edu

Ruihao Gong*
SenseTime Research & Beihang
University
Beijing, Beijing, China
gongruihao@sensetime.com

Tianzi Xiao
SenseTime Research
Beijing, Beijing, China
danache0405@gmail.com

Fengwei Yu
SenseTime Research
Beijing, Beijing, China
yufengwei@sensetime.com

ABSTRACT

Systematic error, which is not determined by chance, often refers to the inaccuracy (involving either the observation or measurement process) inherent to a system. In this paper, we exhibit some long-neglected but frequent-happening adversarial examples caused by systematic error. More specifically, we find the trained neural network classifier can be fooled by inconsistent implementations of image decoding and resize. This tiny difference between these implementations often causes an accuracy drop from training to deployment. To benchmark these real-world adversarial examples, we propose ImageNet-S dataset, which enables researchers to measure a classifier’s robustness to systematic error. For example, we find a normal ResNet-50 trained on ImageNet can have 1%~5% accuracy difference due to the systematic error. Together our evaluation and dataset may aid future work toward real-world robustness and practical generalization.

CCS CONCEPTS

• **Computing methodologies** → **Neural networks**; • **Theory of computation** → *Sample complexity and generalization bounds*.

KEYWORDS

datasets, neural networks, robustness, systematic noise

1 INTRODUCTION

Recently deep learning has shown remarkable success in image recognition [14, 17, 25], speech recognition [13, 19] and natural language processing [4, 8]. However, their security and robustness are greatly challenged by the delicately designed adversarial attacks [6, 12, 20]. The adversarial examples usually fool the neural network without significant visual differences, demonstrating the vulnerability of deep neural networks. This phenomenon attracts broad research interests for different kinds of attacks and defenses.

Currently, the mainstream attack noises can be categorized into adversarial noises and natural noises. The adversarial noises need to be generated according to the model’s specific information such as gradients calculated in backpropagation. Thus, they often achieve satisfactory attack success rates but are rare in real-world scenarios due to the model dependency. In the contrast, there exist natural noises such as blur or corruption [15, 16] that are agnostic to model and frequently encountered in the natural scenario. Although they

have less damage on model robustness compared with adversarial noises, it is impossible to overlook them because of the border range of influence in nature. Therefore, evaluating the robustness of both types of noises is necessary. Some existing defense work [18] surprisingly finds that deep neural networks optimized by adversarial training might be sensitive to natural noises. This indicates that we need diverse noises for a comprehensive understanding of the model’s robustness.

However, the commonly adopted noises are not diverse enough. Besides the man-made noise and natural noise, we point out a new kind of noise-induced by the inconsistent resize or decoder implementation widely existing in the inference system of deep learning model. To be specific, we call it *systematic noise* since they are not corresponded to the model or the input image, but is only related to the inference software and hardware system. Once the software or hardware-software changes, the noise will occur. For example, we always utilize the Pillow package for image decoding and resizing in the PyTorch [21] training system. But when it is deployed on the edge device, it may not support Pillow and we have to seek an alternative for the practical deployment. Sometimes due to the hardware and software’s restriction, the alternative has no way to keep alignment with the origin Pillow implementation, leading to an inevitable systematic noise. The maximum perturbation caused by this systematic noise is only a 1-pixel value but may introduce an obvious accuracy drop (about 1% ~ 5%) in our experiment. Different from the extensively studied adversarial noises and natural noises, this kind of systematic noise is long-term neglected and needs to be included in the robustness evaluation.

In order to attract attention to systematic noise, we summarize the major systematic error sources in the deep learning system and propose a corresponding ImageNet-S dataset, providing provides 3 kinds of decoder noises and 6 kinds of resize noises. It also supports the flexible custom extension by users. We conduct a pioneering benchmark for some prevalent neural architectures on the systematic robustness and find some useful insights: (1) The effect of using different decoders is small while it may have a big impact when using different resize methods; (2) Usually, models in the same architecture will have better robustness of resize with FLOPs (Floating Point Operations) of it get larger, but it doesn’t work for the robustness of decoder; (3) Adversarial methods can increase the robustness of resize method, but we need to find a balance between robustness and clean accuracy. Along with the

*Corresponding Author.

ImageNet-S benchmark dataset, we also propose a simple yet effective mixed training strategy to improve systematic robustness. Our contributions can be summarized as below:

- We firstly indicate a kind of long-neglected but frequent-happening systematic noise caused by the inconsistent deploy software and hardware environment. It may harm the model’s performance in practical application.
- To comprehensively evaluate the effect of systematic noise, we construct an ImageNet-S dataset, which consists of 6 different kinds of resize functions and 3 different kinds of decoder functions. We benchmark the robustness of the prevalent ResNet, RegNetX, MobileNet-V2 networks, and “robust” networks with adversarial training. Even though the systematic noises are slight, they may introduce an up to 2% accuracy jitter, especially for the resize noise.
- To improve the stability when facing systematic noise, we propose a simple yet effective mix training strategy. It can be easily applied in the training routine without much effort but enable the network to enjoy a consistent performance under different deployment systems.

2 RELATED WORK

Adversarial Examples. The adversarial examples were first introduced by [26]. From then on, various adversarial attacks were proposed, such as FGSM [12], PGD [20], C&W [5] and some black-box attack methods [2]. Driven by the emergence of adversarial noises, corresponding defense techniques also arose, including adversarial training [10, 24, 28], data augmentation [11] and regularization [9]. The adversarial examples are always dependent on the model to attack, especially for the block-box attack. Thus they suffer a low transferability and rarely occur in the practical scenario.

Natural Noises. Besides the adversarial examples, the community also realizes the importance of natural noises that are widely existing in the real world. Some representative datasets are constructed to simulate the natural noise, such as ImageNet-P, ImageNet-C [15], and ImageNet-A, ImageNet-O [16]. These noises are model-agnostic and may cause perceptible perturbation. Natural noises such as Snow noise and Frost noise can measure the robustness of a model in the wild.

3 ADVERSARIAL CORRUPTIONS FROM SYSTEMATIC ERROR

In this section, we outline the different system implementations for image decoding and resize. Then, we introduce our ImageNet-S dataset to benchmark the robustness from the different sources of decoding and resizing.

3.1 Notations

Let us denote a RGB image tensor as $X \in [0, 1]^{w \times h \times 3}$ where w and h are the image width and height, respectively. RGB images have 3 channels standing for red, green, and blue colors. However, in computer systems, the images are not stored in this format. Typically there is a raw file (e.g. JPEG) which encodes the tensor X to V . In the case of JPEG encoding, X will be processed by color space conversion, discrete cosine transform (DCT), quantization, and Huffman encoding to V . For image decoding, we should reconstruct

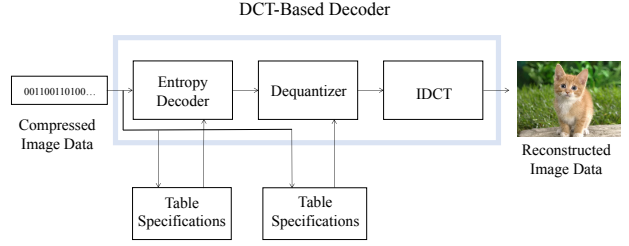


Figure 1: DCT-Based Decoder Processing Steps.

the image tensor X from V . As for image resize, the operation can be represented by $\text{Resize}(X) : [0, 1]^{w \times h \times 3} \rightarrow [0, 1]^{w' \times h' \times 3}$, where w' and h' are the resized width and height, respectively.

Generally, in neural network inference, the image is processed by decoding and resize ($V \rightarrow X \rightarrow X'$)¹. With the different implementations of these two operations, output X' can have different values, which will be discussed in the next two sections.

3.2 Image Decoding

Image decoding refers to the process of translating the raw file (e.g. JPEG) back to an RGB or YUV 3 channel image tensor ($V \rightarrow X$). Image decoding can be divided into several steps: (1) read the raw file from disk as bytes, (2) variable-length decoding (3) zigzag scan, (3) dequantization, (4) inverse discrete cosine transform (iDCT), (5) color conversion and reorder, shown as Figure 1. The fourth step iDCT occupies the majority of the computational cost in the decoding process, which is given by:

$$f[m, n] = \sum_{k=0}^{N-1} \sum_{l=0}^{N-1} \alpha(k)\alpha(l)F(k, l) \cos\left[\frac{(2m+1)\pi k}{2N}\right] \cos\left[\frac{(2n+1)\pi l}{2N}\right] \quad (1)$$

where,

$$\alpha(k) \text{ and } \alpha(l) = \begin{cases} \sqrt{\frac{1}{N}} & \text{if } k = 0 \\ \sqrt{\frac{2}{N}} & \text{if } k \neq 0 \end{cases}$$

In theory, the principle of this process is fixed, but we find decoding one image file in different third-party libraries (e.g. OpenCV [3], Pillow [29], FFmpeg [27]) will output different RGB tensors. This is because they have a unique self-implemented tool to decode the images, especially the iDCT step. We find some libraries prefer to use fast inverse discrete cosine transform (Fast iDCT) instead of the vanilla one, which sacrifices the image quality for the decoding speed. Furthermore, there would be some minor errors in the implementation, such as (ADD EXAMPLES.) These minor errors can cause a shift in the pixel values of the final RGB tensor. Eventually, a single difference in pixel value could fool the neural network to change its prediction. Most of the time, when changing the decoding tools used in training to another one in inference, we observe a drop in accuracy.

¹Sometimes the center crop operation is also utilized. It has a similar impact with the resize operation, therefore we omit its discussion in this paper.

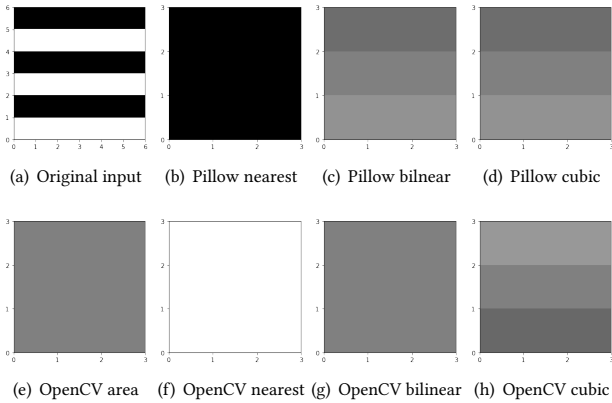


Figure 2: Difference between multi resize methods and tools. Here we visualize the resize output from a synthetic 6×6 image. The first row and the second row contain the Pillow and OpenCV implementation, respectively. We observe the difference not only at the algorithm level but also at the library level.

To evaluate the influence of different image decoders, in Section 4, we will compare with three different decoder tools including OpenCV, Pillow and FFmpeg which are widely used in the field of computer vision.

3.3 Image Resize Method

Image resize is adopted to scale the image resolution to a different size, either up (increase resolution) or down (decrease resolution). In resize operation, one needs to predict the pixel value at an unseen position. This is often performed by different *interpolation* algorithms. We summarize several common algorithms, like nearest neighbor, bilinear, bicubic, etc.

3.3.1 Nearest-neighbor Interpolation. This algorithm, also known as *Proximal Interpolation*, directly selects the value of its nearest known pixel. This mode does not consider the relative magnitude of its neighbor pixels. Therefore, it can preserve sharp details in pixel art, but also introduce jaggedness in previously smooth images [1]. Mathematically, for 2D images where spatial coordinate is represented by (x, y) , the nearest neighbor interpolation will find the existing pixel with lowest Euclidean distance i.e., $X[\arg \min_{x', y'} ((x - x')^2 + (y - y')^2)]$.

3.3.2 Bilinear Interpolation. Bilinear interpolation is a simple extension from linear interpolation by operating on the 2D variables. Unlike Nearest-neighbor algorithm, this mode consider the value of its neighbor and has a rather continuous interpolation effect. Mathematically, our objective is to predict the value of the function $f(\cdot)$ at the unknown point (x, y) . Assume we have four near coordinates: $Q_{11} = (x_1, y_1)$, $Q_{12} = (x_1, y_2)$, $Q_{21} = (x_2, y_1)$, and $Q_{22} = (x_2, y_2)$. Their values are already know, for example $f(Q_{11})$. The formulation of bilinear interpolation is given by:

$$f(x, y) = \frac{y_2 - y}{y_2 - y_1} f(x, y_1) + \frac{y - y_1}{y_2 - y_1} f(x, y_2), \quad (2)$$

Table 1: Image Resize Tools and Their Method.

	Nearest	Bilinear	Cubic	Lanczos	Area	Box	Hamming
OpenCV	✓	✓	✓	✓	✓	✗	✗
Pillow	✓	✓	✓	✓	✗	✓	✓

where,

$$f(x, y_1) = \frac{x_2 - x}{x_2 - x_1} f(Q_{11}) + \frac{x - x_1}{x_2 - x_1} f(Q_{21}),$$

$$f(x, y_2) = \frac{x_2 - x}{x_2 - x_1} f(Q_{12}) + \frac{x - x_1}{x_2 - x_1} f(Q_{22}).$$

3.3.3 Bicubic Interpolation. In contrast to the bilinear interpolation which only takes 4 pixels (2×2), the bicubic interpolation takes 16 pixels (4×4). This method is even more smoothed than bilinear since it considers more neighbors. The algorithm tries to use existing known pixel values to fit a binary cubic function

$$f(x, y) = \sum_{i=0}^3 \sum_{j=0}^3 a_{ij} x^i y^j \quad (3)$$

To find the total 16 coefficients a_{ij} , $ij \in \{0, 1, 2, 3\}$, we need to solve a system of linear equations $A\alpha = x$. Due to the complexity of this algorithm, we refer the readers to this link² for more details. Bicubic interpolation yields better performance than the previous two algorithms, however, it also needs huge time to solve the linear equations to find optimal interpolated values.

3.4 Image Resize Library

We summarize two most commonly used image resize tools in the field of computer vision. Table 1 shows the image resize tools and their corresponding resize method.

Similar to the image decoder, the principal of one kind of image resize method is basically the same, the result will be different due to the difference between implementation detail. Figure 2 shows the difference between resize tools using the same resize method. From this figure, we can see that the gap between different tools using the same method is not small. In the real-world images, different resize tools applying on the same image may not lead to an obvious distance between results, but the gap between them can result in a destabilization of model robustness.

3.5 Visualization of Resize Algorithms

Apart from our mentioned algorithms, many more exists. Here we do not introduce them one by one. To provide an intuitive understanding of the difference, we visualize the results of various resize methods in Figure 2. We use a special 6×6 synthetic image as the original image to magnify the effect of resize. All images are resized to 3×3 resolution. Other interpolation methods like *lanczos*, *area* are also visualized.

Due to the specific characteristics of this synthetic image, we observe a huge disparity between these resize methods. Take the nearest neighbor as an example, this method results in pure color resized images, either whole black (Pillow) or whole white (OpenCV),

²https://www.ece.mcmaster.ca/~xwu/interp_1.pdf

Table 2: Top-1 accuracy of various pre-trained network architectures on ImageNet-S. "N, L, C" refer to nearest neighbor, bilinear, and bicubic resize method. DALI is excluded when calculating the mean and standard deviation.

Architecture	Decode					Resize						
	DALI	OpenCV	Pillow	FFmpeg	Mean \pm Std.	Pillow-N	Pillow-L	Pillow-C	OpenCV-N	OpenCV-L	OpenCV-C	Mean \pm Std.
ResNet-18	70.860	69.720	69.718	69.716	69.718 \pm 2.00E-03	68.906	69.720	70.132	68.842	70.396	70.094	59.728 \pm 6.62E-01
ResNet-34	75.010	74.182	74.176	74.176	74.178 \pm 3.46E-03	73.488	74.182	74.490	73.428	74.834	74.538	63.567 \pm 5.82E-01
ResNet-50	78.140	77.398	77.380	77.408	77.395 \pm 1.42E-02	76.764	77.398	77.736	76.728	77.996	77.858	66.355 \pm 5.54E-01
ResNet-101	79.770	79.110	79.094	79.102	79.102 \pm 8.00E-03	78.386	79.112	79.470	78.660	79.544	79.314	67.785 \pm 4.65E-01
MobileNetV2-0.5	64.938	62.942	62.962	62.976	62.960 \pm 1.71E-02	61.800	62.942	63.494	61.918	63.824	63.518	53.930 \pm 8.68E-01
MobileNetV2-0.75	70.260	68.866	68.870	68.884	68.873 \pm 9.45E-03	67.840	68.866	69.380	67.696	69.608	69.304	58.958 \pm 8.23E-01
MobileNetV2-1	73.120	71.738	71.748	71.734	71.740 \pm 7.21E-03	70.688	71.738	72.158	70.742	72.392	71.948	61.382 \pm 7.27E-01
MobileNetV2-1.4	75.844	74.856	74.824	74.832	74.837 \pm 1.67E-02	73.692	74.856	75.122	73.798	75.396	74.970	63.978 \pm 7.17E-01
RegNetX-200M	68.646	66.866	66.858	66.833	66.852 \pm 1.72E-02	66.048	66.866	67.470	66.014	67.786	67.466	57.380 \pm 7.66E-01
RegNetX-400M	72.220	70.791	70.772	70.776	70.780 \pm 1.00E-02	69.982	70.792	71.204	69.756	71.520	71.348	60.659 \pm 7.40E-01
RegNetX-600M	73.942	72.888	72.896	72.856	72.880 \pm 2.12E-02	71.940	72.888	73.340	71.784	73.676	73.392	62.433 \pm 7.98E-01
RegNetX-800M	75.246	74.338	74.332	74.330	74.333 \pm 4.16E-03	73.458	74.338	74.786	73.394	75.052	74.718	63.679 \pm 7.08E-01
RegNetX-1.6G	77.272	76.570	76.566	76.562	76.566 \pm 4.00E-03	75.858	76.570	77.008	75.728	77.194	76.852	65.603 \pm 6.11E-01

which—as expected—reduces half information. Another major difference comes from the third-party resize libraries. As shown in Fig. 2b and 2g, Pillow and OpenCV have different rounding mechanisms. As a result, they output totally different reversed images. In bicubic interpolation, Pillow and OpenCV also share opposed directions of gradients in color. In practice, the effect of resize operation on real-world images is not as obvious as our example here, however, it is enough to cause wrong predictions for a trained neural network.

4 THE IMAGENET-S ROBUSTNESS BENCHMARK

4.1 ImageNet-S Design

To benchmark the robustness of this unique systematic noise, we aim to build an ImageNet-S dataset. This dataset consists of 3 commonly used decoder types and 6 commonly used resize types. For decoder, we include the implementation from Pillow [29], OpenCV [3] and FFmpeg [27]. For resize operation, we include nearest, cubic and bilinear interpolation modes from both OpenCV and Pillow tools.

To verify the effect of decoding and resize separately, we must fix the decoding method when evaluating the resize and vice versa. In this paper, we set Pillow bilinear mode as the default resize method when testing the decoding robustness. This setting is also the default training setting in PyTorch [21] official code example. Similarly, we set Pillow as the default image decoding tool (same as PyTorch).

We provide not only the validation set of ImageNet with different decoding and resize methods, but also the training set to expose how different decoding and resize methods influence the process of training on a specific model. To enable reproducibility, we save each image file after decoding and resize it as a $3 \times width \times height$ matrix in a .npy file instead of JPEG. According to the commonly used transform on ImageNet [7] train set and test set, we provided two kinds of preprocessing for training and testing respectively. For training, we provide a matrix of an image after random resize crop to $3 \times 224 \times 224$. While for testing, we provide a matrix of an image after the process of resizing to $3 \times 256 \times 256$ then applied a center crop to $3 \times 224 \times 224$.

4.2 Dataset Generator

We provide the generator of ImageNet-S on GitHub³, so that the community can generate system noise dataset and test the robustness of their own models. The basic usage of it is as follows:

```
from imagenet_s_gen import ImageTransfer

ImageTransfer(root_dir='./images/val',
              meta_file='./images/meta/val.txt',
              save_dir='./dataset-decoder-resize',
              decoder_type='pil',
              transform_type=val,
              resize_type='pil-bilinear')
```

5 EXPERIMENTS

Our experiments consist of four parts. First, we evaluate the robustness of existing pre-trained ImageNet models. These models all use the standard [Pillow decoder and Pillow bilinear resize] to train. Second, we study whether the commonly adopted L_2 or L_∞ [5] robust models can defense our ImageNet-S case. Last, we study the training choice of decoding and resize to compare the results on ImageNet-S.

5.1 Network Architecture Experiments

In this section, we test pre-trained neural network models from different architecture to find out the relationship between architecture and systematic noise robustness. Additionally, we aim to find whether the complexity (e.g. FLOPs of the model) of a model can improve the robustness or not. We select architecture from ResNet [14] (including 18, 34, 50, 101 layers models), MobileNetV2 [23] (including width multiplier 0.5, 0.75, 1 and $1.4 \times$ models) and RegNetX [22] (including FLOPs 200, 400, 600, 800, 1600M models). We summarize the results in Table 2 and Figure 3. As can be seen, we find several results: (1) Decoding corruptions are much less obvious than resize corruptions. In the decoding test, we find OpenCV, Pillow and FFmpeg have similar accuracy, with only $< 0.01\%$ accuracy difference. NVIDIA DALI, however, has a moderately different decoding process than these 3 libraries, which generally causes 1%

³<https://github.com/TheGreatCold/ImageNet-S>

Table 3: Top-1 accuracy of various robust ResNet-50 on ImageNet-S.

Robust Type	ϵ	Decode					Resize						
		DALI	OpenCV	Pillow	FFmpeg	Mean \pm Std.	Pillow-N	Pillow-L	Pillow-C	OpenCV-N	OpenCV-L	OpenCV-C	Mean \pm Std.
None	0	75.026	75.616	75.600	75.622	75.613 \pm 1.14E-02	70.626	75.616	75.502	70.624	74.266	72.796	62.780 \pm 2.27E+00
L_2	0.01	75.058	75.386	75.392	75.412	75.397 \pm 1.36E-02	71.490	75.386	75.240	71.578	74.442	73.312	63.067 \pm 1.74E+00
L_2	0.03	75.196	75.538	75.526	75.538	75.534 \pm 6.93E-03	71.614	75.538	75.414	71.562	74.560	73.300	63.145 \pm 1.80E+00
L_2	0.05	75.036	75.240	75.224	75.240	75.235 \pm 9.24E-03	71.740	75.240	75.264	71.732	74.462	73.238	63.100 \pm 1.63E+00
L_2	0.1	74.532	74.558	74.556	74.560	74.558 \pm 2.00E-03	71.390	74.558	74.508	71.344	73.914	72.806	62.649 \pm 1.47E+00
L_2	0.25	74.112	73.730	73.714	73.722	73.722 \pm 8.00E-03	71.384	73.730	73.810	71.328	73.356	72.426	62.293 \pm 1.13E+00
L_2	0.5	73.190	72.476	72.456	72.460	72.464 \pm 1.06E-02	70.366	72.476	72.776	70.422	72.308	71.436	61.400 \pm 1.06E+00
L_2	1	70.548	69.600	69.606	69.606	69.604 \pm 3.46E-03	68.130	69.600	69.976	68.112	69.618	68.956	59.200 \pm 8.02E-01
L_2	3	63.172	61.202	61.194	61.198	61.198 \pm 4.00E-03	60.726	61.202	61.876	60.664	61.664	61.386	52.504 \pm 4.90E-01
L_2	5	56.400	54.292	54.270	54.280	54.281 \pm 1.10E-02	53.900	54.292	54.764	53.880	54.584	54.370	46.542 \pm 3.57E-01
L_∞	0.5/255	73.878	73.246	73.254	73.250	73.250 \pm 4.00E-03	71.040	73.246	73.376	71.102	73.048	72.082	61.987 \pm 1.07E+00
L_∞	1/255	72.298	71.266	71.252	71.256	71.258 \pm 7.21E-03	69.846	71.266	71.594	69.794	71.374	70.690	60.654 \pm 7.88E-01
L_∞	2/255	69.366	68.346	68.350	68.344	68.347 \pm 3.06E-03	67.426	68.346	68.752	67.400	68.562	68.096	58.370 \pm 5.73E-01
L_∞	4/255	63.982	62.518	62.508	62.514	62.513 \pm 5.03E-03	61.458	62.518	63.066	61.542	62.730	62.140	53.352 \pm 6.49E-01
L_∞	8/255	54.854	53.120	53.106	53.124	53.117 \pm 9.45E-03	52.508	53.120	53.508	52.532	53.386	52.990	45.436 \pm 4.20E-01

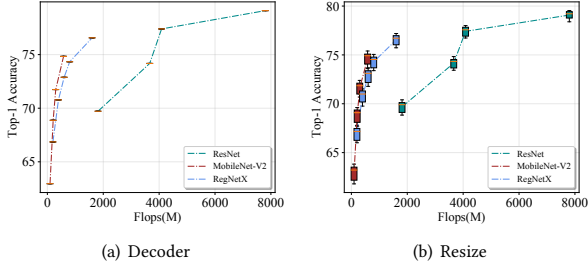


Figure 3: Architecture robustness of systematic noise.

accuracy difference. For resize method, we observe a relatively large gap. The biggest gap for resize operation comes from the nearest neighbor and bilinear interpolation, which generally costs 1 ~ 2% accuracy gap. (2) Different architecture has different robustness, even with similar FLOPs. (3) For models in the same architecture, bigger FLOPs usually result in better robustness in different resize methods. (4) There is no clear relationship between FLOPs and the robustness of different decoders.

5.2 Adversarial Experiments

Adversarial training is a defensive technique that gives model deceptive images during training, thus improving its generalization and robustness. Given a model f_Θ and an input image batch X with the ground truth label Y , an adversarial example of X_{adv} satisfies

$$f_\Theta(x_{adv}) \neq Y \quad s.t. \quad \|X - X_{adv}\|_p \leq \epsilon, \quad (4)$$

where $\|\cdot\|_p$ is a distance metric. Commonly, $\|\cdot\|$ is measured by the ℓ_p -norm ($p \in \{1, 2, \infty\}$).

Adversarial training is one of the most effective approaches to help deep learning models defend against adversarial examples. Thus, it is reasonable to use some adversarial models to test their robustness to our system noise. We download the pre-trained robust trained ResNet-50 [14] from this GitHub repository⁴. The ResNet-50

⁴<https://github.com/microsoft/robust-models-transfer>

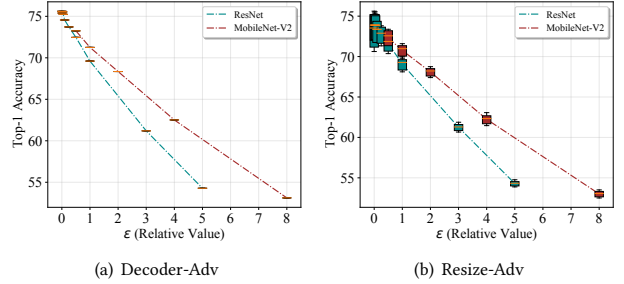


Figure 4: Architecture robustness of systematic noise.

is trained with either L_2 or L_∞ training method. The result is shown in Table 3. We find several interesting insights: (1) Neither of these two adversarial training methods improves the image decoder’s robustness. (2) Both adversarial training methods can improve the robustness of different resize methods. The robustness increase as ϵ gets larger, but a large ϵ would harm the accuracy.

5.3 Robustness Enhancements

As aforementioned, we have verified that adversarial training can enhance resize method robustness, but it cannot help with the robustness on different decoders. This indicates that decoder noise does not belong to the L_p norm perturbation. To overcome this problem, we need other techniques to enhance the systematic robustness.

5.3.1 Mix Training. To solve this problem, a natural way is to make the model “see” all kinds of decoders and resize methods during the training process. Based on this principle, we introduce *mix training* method to enhance the model’s robustness on system noise.

The main process of mix training is to select decoder or resize method randomly instead of just using one kind of method during the whole process of training. The pseudocode of our algorithm is shown in algorithm 1.

Table 4: Mix training on resize method.

Train \ Test	Pillow-bilinear	Pillow-nearest	Pillow-cubic	OpenCV-nearest	OpenCV-bilinear	OpenCV-cubic	Mean	Std.
Pillow-bilinear	76.572	72.168	76.512	72.090	75.346	74.072	74.460	2.02E+00
Pillow-nearest	74.872	75.988	75.548	75.970	76.002	76.056	75.739	4.63E-01
Pillow-cubic	76.312	72.828	76.596	72.876	75.810	74.666	74.848	1.68E+00
OpenCV-nearest	74.818	76.298	75.474	76.092	76.082	76.192	75.826	5.71E-01
OpenCV-bilinear	75.840	75.268	76.446	75.248	76.682	76.436	75.987	6.29E-01
OpenCV-cubic	76.194	72.812	76.510	72.940	75.736	74.818	74.835	1.62E+00
mix	76.154	75.876	76.344	75.786	76.444	76.330	76.156	2.70E-01

Algorithm 1: Mixed training for improving robustness on systematic noise.

Input: Resize set \mathbb{RS} ; Decoder set \mathbb{D} ; Model to train
 Set Pillow-bilinear as default Resize;
 Set Pillow as default Decoder;
for all $j = 1, 2, \dots, T$ -iteration in training **do**
 if use mix-decoder strategy **then**
 Randomly sample a Decoder from \mathbb{D} ;
 if use mix-resize strategy **then**
 Randomly sample a Resize function from \mathbb{RS} ;
 Calling API to load the images from ImageNet-S according to the Decoder type and Resize type;
 Model Optimization.
return An optimized robust model for systematical noise.

model on system noise greatly without hurting the clean accuracy. The *Std.* using mix training drop from 0.36 to 0.0653 on decoder experiment, and drop from 0.463 to 0.270 on resize experiment. Meanwhile, it can maintain the model’s accuracy at about 76%. As a contrast, the same ResNet50 model using L_∞ – Robust adversarial training drop the *Std.* from 1.07 to 0.420 by paying 19.2% drop of clean accuracy.

6 CONCLUSION

In this paper, we introduced what is to our knowledge the first dataset, ImageNet-S, for real-world robustness from systematic noise. We focused on a problem that exists in the process of practical application, but it is easy to be ignored in practice. We finished lots of experiments that do show that the difference between different decoders and resize methods can influence on model’s accuracy. Therefore, we used mean and standard deviation which are used to measure the robustness of systematic noise. With this matrix, we did experiments and found the relation between architecture, adversarial, and the robustness of a model. What’s more, we found a way called mix training to enhance the system noise robustness without hurting the clean accuracy.

Table 5: Mix training on decoder.

Train \ Test	Pillow	OpenCV	FFmpeg	Mean	Std.
Pillow	76.430	76.426	75.310	76.055	6.45E-01
OpenCV	76.510	76.510	75.368	76.126	6.56E-01
FFmpeg	75.730	75.664	76.318	75.904	3.60E-01
mix	76.53	76.524	76.414	76.489	6.53E-02

To test the effect of mix training, we set up the following experiment. We use ResNet50 as the base model of this experiment. To comprehensively demonstrate the training effect, we train single decoding and resize as well as our mix training models. We set the default decoder as Pillow and the default resize method as Pillow bilinear when conducting ablation studies on resize method or decoder, respectively. Then we use top-1 accuracy as well as their mean and standard deviation as assessments.

The results of this experiment are shown in Table 5 and Table 4. From these tables, we can know that: (1) The model has a better performance (usually the best) when we train and test using the same decoder and resize method. (2) There is a big gap when we train and test the same model using different methods. For example, the accuracy of ResNet50 trained by Pillow bilinear method is about 2.4% lower than that trained by OpenCV bilinear on the test set which is resized by OpenCV cubic. While, on the whole, the gap between different decoders is smaller than that between different resize methods. (3) Mix training can improve the robustness of a

REFERENCES

- [1] 2017. Nearest-neighbor interpolation. https://en.wikipedia.org/wiki/Nearest-neighbor_interpolation
- [2] Arjun Nitin Bhagoji, Warren He, Bo Li, and Dawn Song. 2018. Practical Black-box Attacks on Deep Neural Networks using Efficient Query Mechanisms. In *Proceedings of the European Conference on Computer Vision (ECCV)*.
- [3] G. Bradski. 2000. The OpenCV Library. *Dr. Dobb's Journal of Software Tools* (2000).
- [4] Tom Brown, Benjamin Mann, Nick Ryder, Melanie Subbiah, Jared D Kaplan, Prafulla Dhariwal, Arvind Neelakantan, Pranav Shyam, Girish Sastry, Amanda Askell, Sandhini Agarwal, Ariel Herbert-Voss, Gretchen Krueger, Tom Henighan, Rewon Child, Aditya Ramesh, Daniel Ziegler, Jeffrey Wu, Clemens Winter, Chris Hesse, Mark Chen, Eric Sigler, Mateusz Litwin, Scott Gray, Benjamin Chess, Jack Clark, Christopher Berner, Sam McCandlish, Alec Radford, Ilya Sutskever, and Dario Amodei. 2020. Language Models are Few-Shot Learners. In *Advances in Neural Information Processing Systems*, H. Larochelle, M. Ranzato, R. Hadsell, M. F. Balcan, and H. Lin (Eds.), Vol. 33. Curran Associates, Inc., 1877–1901.
- [5] Nicholas Carlini and David Wagner. 2017. Towards evaluating the robustness of neural networks. In *2017 IEEE Symposium on Security and Privacy (SP)*. IEEE, 39–57.
- [6] Francesco Croce and Matthias Hein. 2020. Reliable evaluation of adversarial robustness with an ensemble of diverse parameter-free attacks. In *ICML*.
- [7] J. Deng, W. Dong, R. Socher, L.-J. Li, K. Li, and L. Fei-Fei. 2009. ImageNet: A Large-Scale Hierarchical Image Database. *2009 IEEE Conference on Computer Vision and Pattern Recognition (CVPR)* (Jul 2009).
- [8] Jacob Devlin, Ming-Wei Chang, Kenton Lee, and Kristina Toutanova. 2018. BERT: Pre-training of Deep Bidirectional Transformers for Language Understanding. *arXiv preprint arXiv:1810.04805* (2018).
- [9] Chaohao Fu, Hongbin Chen, Na Ruan, and Weijia Jia. 2020. Label Smoothing and Adversarial Robustness. *arXiv preprint arXiv:2009.08233* (2020).
- [10] Yaroslav Ganin, Evgeniya Ustinova, Hana Ajakan, Pascal Germain, Hugo Larochelle, François Laviolette, Mario Marchand, and Victor Lempitsky. 2016. Domain-adversarial training of neural networks. *The journal of machine learning research* 17, 1 (2016), 2096–2030.
- [11] Chengyue Gong, Tongzheng Ren, Mao Ye, and Qiang Liu. 2021. MaxUp: Lightweight Adversarial Training With Data Augmentation Improves Neural Network Training. In *Proceedings of the IEEE/CVF Conference on Computer Vision and Pattern Recognition (CVPR)*. 2474–2483.
- [12] Ian J Goodfellow, Jonathon Shlens, and Christian Szegedy. 2014. Explaining and harnessing adversarial examples. *arXiv preprint arXiv:1412.6572* (2014).
- [13] Wei Han, Zhengdong Zhang, Yu Zhang, Jiahui Yu, Chung-Cheng Chiu, James Qin, Anmol Gulati, Ruoming Pang, and Yonghui Wu. 2020. Contextnet: Improving convolutional neural networks for automatic speech recognition with global context. *arXiv preprint arXiv:2005.03191* (2020).
- [14] Kaiming He, Xiangyu Zhang, Shaoqing Ren, and Jian Sun. 2016. Deep Residual Learning for Image Recognition. In *Proceedings of the IEEE Conference on Computer Vision and Pattern Recognition (CVPR)*.
- [15] Dan Hendrycks and Thomas Dietterich. 2019. Benchmarking Neural Network Robustness to Common Corruptions and Perturbations. *Proceedings of the International Conference on Learning Representations* (2019).
- [16] Dan Hendrycks, Kevin Zhao, Steven Basart, Jacob Steinhardt, and Dawn Song. 2021. Natural Adversarial Examples. *CVPR* (2021).
- [17] Alex Krizhevsky, Ilya Sutskever, and Geoffrey E Hinton. 2012. ImageNet Classification with Deep Convolutional Neural Networks. In *Advances in Neural Information Processing Systems 25*, F. Pereira, C. J. C. Burges, L. Bottou, and K. Q. Weinberger (Eds.), Curran Associates, Inc., 1097–1105.
- [18] Alfred Laugros, Alice Caplier, and Matthieu Ospici. 2019. Are adversarial robustness and common perturbation robustness independent attributes?. In *Proceedings of the IEEE/CVF International Conference on Computer Vision Workshops*. 0–0.
- [19] Jason Li, Vitaly Lavrukhin, Boris Ginsburg, Ryan Leary, Oleksii Kuchaiev, Jonathan M Cohen, Huyen Nguyen, and Ravi Teja Gadde. 2019. Jasper: An end-to-end convolutional neural acoustic model. *arXiv preprint arXiv:1904.03288* (2019).
- [20] Aleksander Madry, Aleksandar Makelov, Ludwig Schmidt, Dimitris Tsipras, and Adrian Vladu. 2018. Towards Deep Learning Models Resistant to Adversarial Attacks. *Proceedings of the International Conference on Learning Representations* (2018).
- [21] Adam Paszke, Sam Gross, Soumith Chintala, Gregory Chanan, Edward Yang, Zachary DeVito, Zeming Lin, Alban Desmaison, Luca Antiga, and Adam Lerer. 2017. Automatic differentiation in PyTorch. (2017).
- [22] Ilija Radosavovic, Raj Prateek Kosaraju, Ross Girshick, Kaiming He, and Piotr Dollar. 2020. Designing Network Design Spaces. In *Proceedings of the IEEE/CVF Conference on Computer Vision and Pattern Recognition (CVPR)*.
- [23] Mark Sandler, Andrew Howard, Menglong Zhu, Andrey Zhmoginov, and Liang-Chieh Chen. 2018. MobileNetV2: Inverted Residuals and Linear Bottlenecks. In *Proceedings of the IEEE Conference on Computer Vision and Pattern Recognition (CVPR)*.
- [24] Ali Shafahi, Mahyar Najibi, Amin Ghiasi, Zheng Xu, John Dickerson, Christoph Studer, Larry S Davis, Gavin Taylor, and Tom Goldstein. 2019. Adversarial training for free! *arXiv preprint arXiv:1904.12843* (2019).
- [25] Karen Simonyan and Andrew Zisserman. 2014. Very deep convolutional networks for large-scale image recognition. *arXiv preprint arXiv:1409.1556* (2014).
- [26] Christian Szegedy, Wojciech Zaremba, Ilya Sutskever, Joan Bruna, Dumitru Erhan, Ian Goodfellow, and Rob Fergus. 2013. Intriguing properties of neural networks. *arXiv preprint arXiv:1312.6199* (2013).
- [27] Suramya Tomar. 2006. Converting video formats with FFmpeg. *Linux Journal* 2006, 146 (2006), 10.
- [28] Florian Tramèr, Alexey Kurakin, Nicolas Papernot, Ian Goodfellow, Dan Boneh, and Patrick McDaniel. 2017. Ensemble adversarial training: Attacks and defenses. *arXiv preprint arXiv:1705.07204* (2017).
- [29] P Umesh. 2012. Image Processing in Python. *CSI Communications* 23 (2012).